PTEP

Prog. Theor. Exp. Phys. **2014**, 113D03 (12 pages)
DOI: 10.1093/ptep/ptu155

A systematic study of even–even nuclei from Ne to Ca in covariant density functional theory with triaxiality

Ying Wang[1], Jian Li[1,*], Jing Bin Lu[1,*], and Jiang Ming Yao[2,3]

[1]*College of Physics, Jilin University, Changchun 130012, China*
[2]*Department of Physics, Tohoku University, Sendai 980-8578, Japan*
[3]*School of Physical Science and Technology, Southwest University, Chongqing 400715, China*
[*]E-mail: jianli@jlu.edu.cn, ljb@jlu.edu.cn

Received April 28, 2014; Revised October 9, 2014; Accepted October 15, 2014; Published November 19, 2014

The ground-state properties of even–even nuclei from $Z = 10$ to $Z = 20$ are systematically studied in covariant density functional theory with the point-coupling interaction PC-PK1. The triaxiality effect on nuclear binding energy, including the mean-field part and rotational correction energy, is examined. We find that ^{38}Si, ^{46}S, and ^{48}S exhibit considerable triaxial deformation. The results indicate that the static effect from the triaxial deformation degree of freedom on the mean-field part of the nuclear binding energy in the present nuclei is marginal; however, it has a significant effect on the rotational correction energy. Moreover, we show that the root-mean-square deviation in binding energies for the 41 nuclei from Ne to Ar is reduced from 2.22 MeV to 1.60 MeV and the evolution trend of the $N = 20$ shell gap is better reproduced after considering phenomenological collective correction.

Subject Index D04, D11, D12

1. Introduction

In recent years, the radioactive ion beam (RIB) has provided the possibility of studying the structural properties of nuclei far from stability. The neutron-rich nuclei in the light-mass region are of particular interest. Many novel phenomena have been observed, such as halo phenomena [1], the island of inversion [2], neutron skins [3], new magic number [4], and the decoupling structure of the halo from the "core" nucleus [5].

On the theoretical side, various methods have been applied to study the structure of nuclei in the light-mass region. Density functional theory (DFT) is the only tractable microscopic theory that can be applied for large-scale nuclear structure calculations across the entire table of nuclides with a universal energy density functional (EDF) [6–8]. Within this framework, the covariant density functional theory (CDFT), based on an effective relativistic Lagrangian, has achieved great success in the description of ground-state properties of both spherical and deformed nuclei all over the nuclear chart [6,9–13].

In the past decades, the relativistic mean-field (RMF) implementation of the CDFT framework has been applied to systematic investigations of light nuclei by allowing the nuclei to be axially deformed [14–17]. However, the influence of the triaxiality effect has not been examined. A specific combination of single-particle orbitals near the Fermi surface and the additional binding energy from

nonaxial degrees of freedom can enhance the tendency to form nuclei with triaxial shapes. Several islands of triaxiality have been revealed throughout the nuclear chart [18]. The inclusion of triaxiality can dramatically reduce the barrier separating prolate and oblate minima, leading to structures that are soft or unstable for triaxial distortions [19]. Furthermore, the occurrence of triaxiality can give rise to many very interesting modes of collective motion. The RMF approach with triaxiality was firstly developed by Koepf and Ring [20]. Later on, Hirata et al. carried out a systematic calculation of S isotopes and found γ-soft or triaxial deformation in some nuclei [21]. Subsequently, some systematic studies of triaxial deformation in the RMF approach have been performed in different mass regions [22–24]. In particular, Yao et al. recently performed a beyond-RMF study of Mg isotopes, and found that the triaxiality effect on the low-lying states is marginal for most Mg isotopes, except for ^{26}Mg [25].

In recent years, the CDFT with a point-coupling effective Lagrangian has attracted a lot of attention. In this framework, a new parametrization, PC-PK1, was proposed [26], which provides a good description of the isospin dependence of binding energy along either the isotopic or the isotonic chain. In particularly, after taking into account the rotational correction energy in the cranking approximation, PC-PK1 achieves the same quality as DD-PC1, which is adjusted to the binding energies of 64 well deformed nuclei, in the description of deformed nuclei, including both the binding energy and deformation. Recently, after including the collective corrections on top of axially deformed RMF calculations using the PC-PK1 force, the root-mean-square (rms) deviation for the masses of 575 even–even nuclei ranging from $Z = 8$ to $Z = 108$ was reduced from 2.58 MeV to 1.24 MeV [27]. The remaining deviation is mainly contributed from the light nuclei. For nuclei with proton numbers $8 < Z < 20$, the rms deviation in mass turns out to be 2.18 MeV. Therefore, the nuclei in this mass region require further dedicated investigation. It is natural to ask the question of how large the effect of triaxial deformation is in the binding energies of light nuclei.

The aim of this work is to examine the triaxiality effect in the ground-state properties of even–even nuclei with proton numbers from $Z = 10$ to $Z = 20$. To this end, we carry out a systematic study with a triaxial RMF approach using the PC-PK1 force. The deformation energy surface, quadrupole and triaxial deformation parameters, and binding energies will be presented. The effects of triaxiality and collective correction on nuclear binding energy and the $N = 20$ shell gap will be discussed.

2. Theoretical framework

In the point-coupling type of CDFT, the energy density functional for a nuclear system has the following form [26,28,29]:

$$E_{\mathrm{DF}} = \int d^3r \mathcal{E}(\boldsymbol{r}) \tag{1}$$

with the energy density

$$\begin{aligned}\mathcal{E}(\boldsymbol{r}) = &\sum_k v_k^2 \psi_k^\dagger(\boldsymbol{r})(\boldsymbol{\alpha}\cdot\boldsymbol{p} + \beta m)\psi_k(\boldsymbol{r}) \\ &+ \frac{\alpha_S}{2}\rho_S^2 + \frac{\beta_S}{3}\rho_S^3 + \frac{\gamma_S}{4}\rho_S^4 + \frac{\delta_S}{2}\Delta\rho_S \\ &+ \frac{\alpha_V}{2}\rho_V^2 + \frac{\gamma_V}{4}\rho_V^4 + \frac{\delta_V}{2}\rho_V\Delta\rho_V \\ &+ \frac{\alpha_{TV}}{2}\rho_{TV}^2 + \frac{\delta_{TV}}{2}\rho_{TV}\Delta\rho_{TV} + \frac{1}{2}eA_0\rho_V^p.\end{aligned} \tag{2}$$

Here, m is the nucleon mass, and α_S, α_V, α_{TV}, β_S, γ_S, γ_V, δ_S, δ_V, and δ_{TV} are coupling constants. Moreover, A_μ is the four-vector potential for the electromagnetic field and $\rho_i (i = S, V, TS, TV)$ represents various local densities. The subscripts S, V, and T indicate the symmetries of the couplings, i.e., S stands for scalar, V for vector, T for isovector, respectively.

For open-shell nuclei, pairing correlations are taken into account using the Bardeen-Cooper-Schrieffer (BCS) method with a density-independent δ force and the pairing energy has the following form:

$$E_{\text{pair}} = -\sum_{\tau=n,p} \frac{V_\tau}{4} \int d^3r \kappa_\tau^*(\boldsymbol{r}) \kappa_\tau(\boldsymbol{r}), \tag{3}$$

where V_τ is the constant pairing strength, adjusted by fitting the average single-particle pairing gap. The pairing tensor reads

$$\kappa(\boldsymbol{r}) = -2 \sum_{k>0} f_k u_k v_k |\psi_k(\boldsymbol{r})|^2, \tag{4}$$

with the smooth-cutoff weight factor f_k [30,31]. In addition, v_k^2 stands for the occupation probability of the kth single-particle state.

We note here that the BCS method can provide results for most nuclei very close to those of the Hartree–(Fock)–Bogoliubov (HFB) approach [32,33], except for the drip-line nuclei with halo structure. Considering that the main purpose of the present study is to examine the triaxiality effect on binding energies of nuclei with available data, instead of predicting the nucleon drip-line, which has been studied very recently with the relativistic (continuum) Hartree–Bogoliubov approach in Refs. [34,35], and is beyond the scope of the present study, the BCS method provides an economic way to take into account the pairing correlation and is thus adopted in the present study.

Because of the breaking of translational symmetry by the mean-field approximation, the energy from the center-of-mass (c.m.) correction is evaluated as follows [31,36]:

$$E_{\text{c.m.}} = -\frac{1}{2mA} \left\langle \hat{\boldsymbol{P}}_{\text{c.m.}}^2 \right\rangle, \tag{5}$$

where A is the mass number and $\hat{\boldsymbol{P}}_{\text{c.m.}} = \sum_i^A \hat{\boldsymbol{p}}_i$ is the total momentum in the c.m. frame.

Finally, the total energy for the nuclear system becomes

$$E_{\text{tot}} = E_{\text{DF}} + E_{\text{pair}} + E_{\text{c.m.}}. \tag{6}$$

The potential energy surface (PES) in the plane of deformation variables (β, γ) is obtained by adding a quadratic constraint on the mass quadrupole moments to the total energy during the variation [37],

$$\sum_{\mu=0,2} C_{2\mu} (\langle \hat{Q}_{2\mu} \rangle - q_{2\mu})^2, \tag{7}$$

where $C_{2\mu}$ is an arbitrary stiffness constant and $q_{2\mu}$ is the desired value of the quadrupole moments. $\langle \hat{Q}_{2\mu} \rangle$ is the expectation value of the mass quadrupole operator,

$$\hat{Q}_{20} = 2z^2 - x^2 - y^2, \tag{8}$$

$$\hat{Q}_{22} = x^2 - y^2. \tag{9}$$

The triaxial deformation parameters β and γ are related to the values of $\langle \hat{Q}_{20} \rangle$ and $\langle \hat{Q}_{22} \rangle$ by

$$\langle \hat{Q}_{20} \rangle = \frac{3A}{4\pi} R_0^2 \beta \cos\gamma, \tag{10}$$

$$\langle \hat{Q}_{22} \rangle = \frac{3A}{4\pi} R_0^2 \frac{1}{\sqrt{2}} \beta \sin\gamma, \tag{11}$$

where $R_0 = 1.2A^{1/3}$ fm.

3. Results and discussion

There are no parameters in our study other than those in the EDF (2), for which the relativistic point-coupling parametrization PC-PK1 [26] is used throughout this work. The pairing strengths have been adjusted by fitting the average single-particle pairing gap to the empirical neutron pairing gaps for ^{122}Sn, ^{124}Sn, and ^{200}Pb as well as the proton ones for ^{92}Mo, ^{136}Xe, and ^{144}Sm obtained with the five-point formula in Ref. [26]. The solution of the Dirac equation for nucleons is accomplished by an expansion of the Dirac spinors in a set of 3D harmonic oscillator basis functions in Cartesian coordinates with 10 major shells, which are found to obtain reasonably converged results for the nuclei concerned. More details about the calculations can be found in Ref. [38]. To find out the actual mean-field ground state, we carry out the constraint calculations with varying deformation parameters (β, γ), $\beta \in [0.0, 0.6]$ and $\gamma \in [0^\circ, 60^\circ]$ with step size $\Delta\beta = 0.05$ and $\Delta\gamma = 5^\circ$, to obtain the energy surface. After that, we solve the Dirac equation iteratively without constraint starting from the configuration of the lowest energy obtained in the constraint calculation until self-consistent convergence is achieved.

3.1. *Potential energy surfaces and deformation parameters*

As an example, we plot the potential energy surfaces of the even–even $^{26-56}$S isotopes in the β–γ plane from the constrained RMF+BCS calculation in Fig. 1. It provides a clear picture for the ground-state evolution in the β–γ plane from ^{26}S to ^{56}S. The most neutron-deficient nucleus ^{26}S is spherical, but somewhat soft, while ^{28}S is very soft along the β direction in the region with $0 < \beta < 0.4$. With the increase of neutron number up to $N = 20$, the nucleus gradually becomes spherical. As the neutron number increases further, the nucleus becomes prolate deformed with quadrupole deformation $\beta = 0.25$. A prolate-deformed ground state with γ-soft is observed in ^{44}S with traditional neutron magic number $N = 28$, which has been discussed in detail in Ref. [39]. A triaxial minimum with $\gamma \simeq 30^\circ$ is exhibited in ^{46,48}S. However, this triaxial minimum is also soft along the γ direction. The nucleus becomes gradually spherical again when the neutron number increases further up to $N = 40$. In Ref. [21], the energy surfaces in ^{42,44,46,48,50,52,54,56}S have been given by the triaxial RMF calculation using the TM1 force [40] and the corresponding shape evolution has been studied. However, there are some differences in detail. For instance, the TM1 force predicted ^{42}S to have two competing prolate and oblate minima, which are separated by a barrier along the γ direction, instead of a single prolate-deformed minimum by the PC-PK1 force. For ^{50}S, the TM1 force gave a deformed ground state with $\beta = 0.25$ and γ being extremely flat, instead of the spherical minimum by the PC-PK1 force. We note that ^{46,48}S are predicted to be triaxially deformed by both forces.

Figure 2 displays the deformation parameters β and γ corresponding to the minima of the energy surfaces for the nuclei concerned. The upper panel shows that the β value is zero for the nuclei with neutron magic numbers $N = 8$ and $N = 20$, but nonzero for $N = 28$. The $N = 28$ isotopes with $Z < 20$ exhibit deformed ground states, which was noticed many years ago [6] and has been discussed in detail recently with a 5D collective Hamiltonian on top of the CDFT in Ref. [39]. In addition, $\beta < 0.3$ is found for most nuclei, with the exception of some Ne and Mg isotopes, i.e., ^{20,22,32,34}Ne and ^{22,24,34,36,38,40}Mg, which have large quadrupole deformation ($\beta > 0.4$). In Ref. [41], a global study of nuclear ground-state properties has been performed with the HFB approach using the Gogny D1S force. We note that our results show some similarities with the Gogny-HFB calculated results. Specifically, the $N = 8$ and $N = 20$ isotones are predicted to be spherical in both calculations. For the $N = 28$ isotones, the deformation β of ^{42}Si and ^{44}S is considerable, while

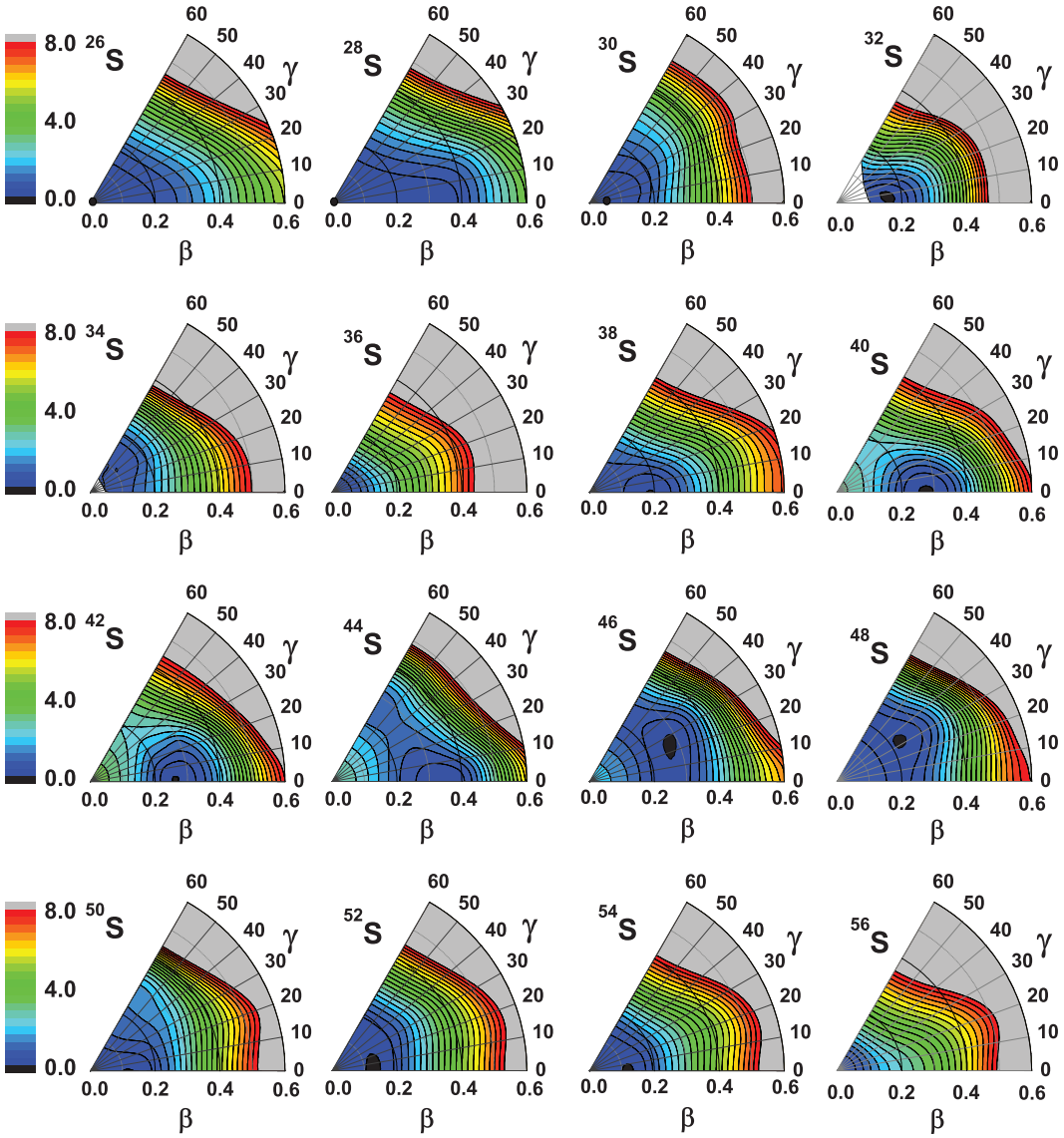

Fig. 1. Potential energy surfaces of even–even $^{26-56}$S isotopes in the β–γ plane from the triaxial RMF calculation with the PC-PK1 force. All energies are normalized with respect to the global minimum. The energy difference between neighboring contour lines is 0.4 MeV.

β of ^{46}Ar is zero. Moreover, $\beta < 0.3$ is also found for most nuclei in the Gogny-HFB calculations, except ^{20,22,34}Ne and ^{22,24,34,36}Mg, which were predicted to have large quadrupole deformation ($\beta > 0.4$).

The lower panel of Fig. 2 shows that the Ne, Mg, and S isotopes are mostly prolate deformed, while the Si and Ar isotopes are in most cases oblate deformed. Some Si and S isotopes exhibit rapid shape transition and even the coexistence of prolate, oblate, and triaxial deformations. In total, there are 8 nuclei with triaxial deformation, among which ^{38}Si, ^{46}S, and ^{48}S exhibit considerable triaxial deformation. However, the triaxial effect has an evident effect only on ^{48}S, increasing the deformation parameter β from 0.2 to 0.25 and the binding energy by 0.15 MeV. For the other two nuclei, the triaxial effect is negligible for nuclear binding energy. The rms deviations of binding energies for the 41 nuclei ranging from Ne to Ar turn out to be 2.22 MeV irrespective of whether the triaxiality is taken into account or not at the mean-field level. This indicates that the static effect from

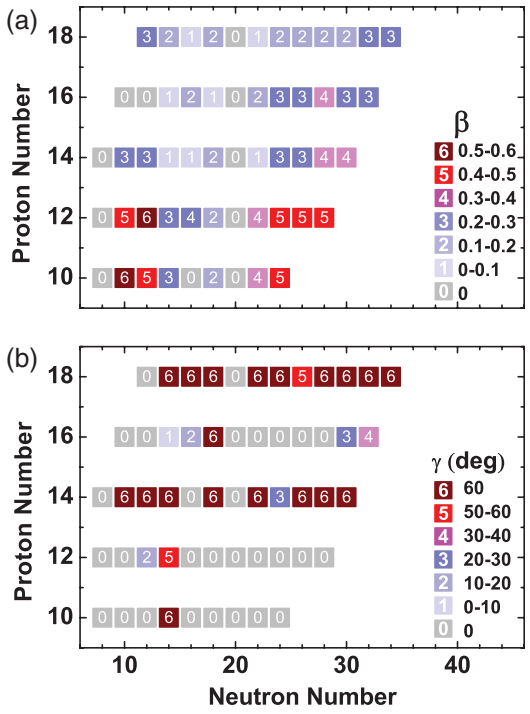

Fig. 2. The quadrupole deformation parameters β (a) and γ (b) for the ground states of nuclei with proton numbers $10 \leq Z \leq 18$ from the triaxial RMF calculations with the PC-PK1 force. The sizes of β and γ are indicated with numbers.

the triaxial deformation degree of freedom is marginal for the light nuclei in present relativistic mean-field calculations. In the Gogny-HFB calculations [41], there are 10 nuclei with triaxial deformation on the whole, among which 7 nuclei have small quadrupole deformation ($\beta < 0.05$) or small triaxial deformation ($\gamma < 5^\circ$ or $55^\circ < \gamma < 60^\circ$). The corresponding deformation parameters (β, γ) for the remaining 3 nuclei ^{24}Ne, ^{24}Si, and ^{44}Ar are $(0.22, 52^\circ)$, $(0.23, 47^\circ)$, and $(0.08, 11^\circ)$, respectively.

It should be noted that experimental information, such as the precise mass measurements [42] and/or the observations of low-lying first excited states with large $B(E2)$ transition probabilities (see, e.g., Ref. [43] and references therein), shows that the neutron magic number $N = 20$ in the neutron-rich nuclei is broken (or quenched) and it is related to the appearance of a deformed ground state. For example, the quadrupole deformation of ^{32}Mg extracted from experimental $B(E2 : 0^+ \rightarrow 2^+)$ can be as large as $\beta \simeq 0.5$. This region around $N = 20$ is sometimes also referred to as the "island of inversion" [2]. However, it is well known that mean-field theories, including the RMF calculations [14,17,44] and non-relativistic Hartree–Fock–Bogoliubov calculations [41,45], cannot give large deformations for neutron-rich nuclei with $N = 20$, such as ^{30}Ne and ^{32}Mg. The understanding of this exotic phenomenon requires beyond-mean-field studies, which are beyond the scope of the present study.

3.2. *Effects of rotational correction energy*

For deformed nuclei, the rotational symmetry is broken in the mean-field solution. In this case, the correction from the restoration of rotational symmetry has to be taken into account. Since the exact angular momentum projection (AMP) calculation is time-consuming, one can evaluate the rotational

correction energy (RCE) with triaxial deformation in the following simple way [37]:

$$E^{\rm rot} = \frac{1}{2}\left[\frac{\langle \hat{J}_x^2\rangle}{\mathcal{I}_x} + \frac{\langle \hat{J}_y^2\rangle}{\mathcal{I}_y} + \frac{\langle \hat{J}_z^2\rangle}{\mathcal{I}_z}\right], \tag{12}$$

where $\hat{J}_{x(y,z)}$ is the angular momentum operator. $\mathcal{I}_{x(y,z)}$ could be either the Thouless–Valatin moment of inertia derived from time-dependent mean-field approaches or the Peierls–Yoccoz moment of inertia derived from projection after variation methods. For the sake of simplicity, people usually calculate $\mathcal{I}_{x(y,z)}$ using the Inglis–Belyaev formula [46,47], which is equivalent to the Thouless–Valatin moment of inertia in the case without residual interaction [48]. This prescription has been adopted extensively in the mass formulae [49–51]. However, the Inglis–Belyaev formula is well known to underestimate the moment of inertia by about 30% and is not suitable for nuclei close to spherical shape. In addition, it has been shown in Refs. [52,53] that the rotational correction energy calculated by Eq. (12) deviates significantly from the exact angular momentum projection results for deformed nuclei, and even becomes very large for some weakly deformed nuclei. In view of these facts, the phenomenological collective correction is adopted, i.e., one usually introduces a deformation-dependent quenching factor to cure this problem [49–51],

$$E^{\rm corr} = E^{\rm rot} \cdot b\tanh(c|\beta|), \tag{13}$$

with β the calculated quadrupole deformation. Here, the parameters b, c are fitted to the discrepancy between the experimental binding-energy data and the mean-field values. They are found to be close to the corresponding parameters $b = 0.80$ and $c = 10$ in Ref. [51], which are also used in Ref. [27]. Therefore, these values will be adopted in the following calculations. In Ref. [27], an additional term representing the deformation dependence of the vibrational correction is adopted for the corrections and the dynamical correlation energy is called for, including both rotational and vibrational corrections. Based on the Generator Coordinate Method calculation, the collective correction energy is dominated by the rotational part [25,54]. Therefore, for the sake of simplicity, the vibrational contribution is not included in this work.

As the three nuclei ^{38}Si, ^{46}S, and ^{48}S have considerable triaxial deformation, to demonstrate the triaxial deformation effects, Fig. 3 displays their rotational correction energies in the β–γ plane calculated by Eq. (12) with triaxial RMF wavefunctions. It is easy to see that, for these three nuclei, the rotational correction energies increase with β in the area with considerable γ. In the area with γ close to 0° or 60°, the rotational correction energies become more sensitive to γ, and show a drastic decrease. Taking ^{38}Si as an example, the ground-state rotational correction energies are 3.83 MeV

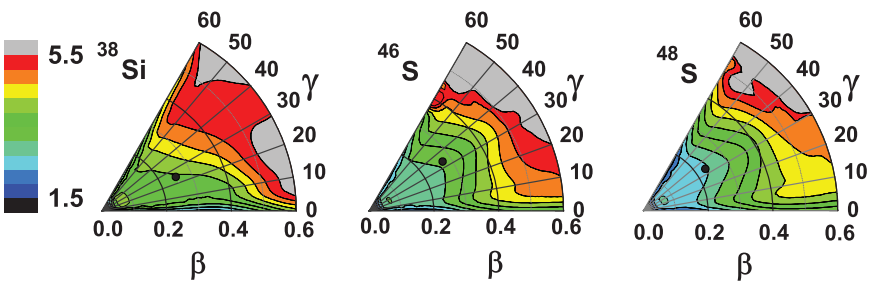

Fig. 3. The rotational correction energies of ^{38}Si, ^{46}S, and ^{48}S in the β–γ plane calculated by Eq. (12) with triaxial RMF wavefunctions. The contours join points on the surface with the same energy. The difference between neighboring contours is 0.4 MeV.

($\beta = 0.25$, $\gamma = 24^\circ$) and 1.95 MeV ($\beta = 0.3$, $\gamma = 0^\circ$), respectively with and without considering the triaxial deformation freedom. Thus, for ^{38}Si, the ground-state rotational correction energies will be increased by about 1.9 MeV, with considering the triaxial deformation freedom, while the corresponding values will be 0.8 and 0.2 MeV, respectively, for ^{46}S and ^{48}S.

To clearly illustrate the effect of the triaxial deformation degree of freedom on rotational correction energies, taking ^{38}Si as an example, the three components ($i = x, y, z$) for the expectation of the square of angular momentum $\langle \hat{J}_i^2 \rangle$, moment of inertia $\mathcal{I}_i$, and rotational correction energies $\langle \hat{J}_i^2 \rangle / \mathcal{I}_i$ in the β–γ plane are given in Fig. 4. It is easy to see that $\langle \hat{J}_x^2 \rangle$ increases remarkably with the quadrupole deformation, while $\langle \hat{J}_y^2 \rangle$ and $\langle \hat{J}_z^2 \rangle$ strongly depend on the triaxial deformation. Moreover, $\langle \hat{J}_y^2 \rangle$ decreases to zero when γ is approaching 60°, and $\langle \hat{J}_z^2 \rangle$ decreases to zero when γ is approaching 0°. For the moment of inertia, $\mathcal{I}_x$ depends more on β with relatively small quadrupole deformation, and it becomes sensitive to γ in the area with relatively large β. In addition, both $\mathcal{I}_y$ and $\mathcal{I}_z$ are very sensitive to γ, and they show almost the same trend as $\langle \hat{J}_y^2 \rangle$ and $\langle \hat{J}_z^2 \rangle$, respectively, in the β–γ plane. For the above reasons, $\langle \hat{J}_x^2 \rangle / \mathcal{I}_x$ is sensitive to both β and γ, while $\langle \hat{J}_y^2 \rangle / \mathcal{I}_y$ and $\langle \hat{J}_z^2 \rangle / \mathcal{I}_z$ are more sensitive to γ. Finally, it is easy to understand from Fig. 4 that triaxiality plays a decisive role in the increase of the rotational correction energies in ^{38}Si with ground state from $\beta = 0.3$, $\gamma = 0^\circ$ to $\beta = 0.25$, $\gamma = 24^\circ$. In short, only two terms in Eq. (12) are nonzero in the axial case ($\gamma = 0^\circ$ or $\gamma = 60^\circ$), while all three terms are nonzero in the triaxial case. In general, although the triaxial deformation degree of freedom has a tiny effect on the energies of the mean-field ground

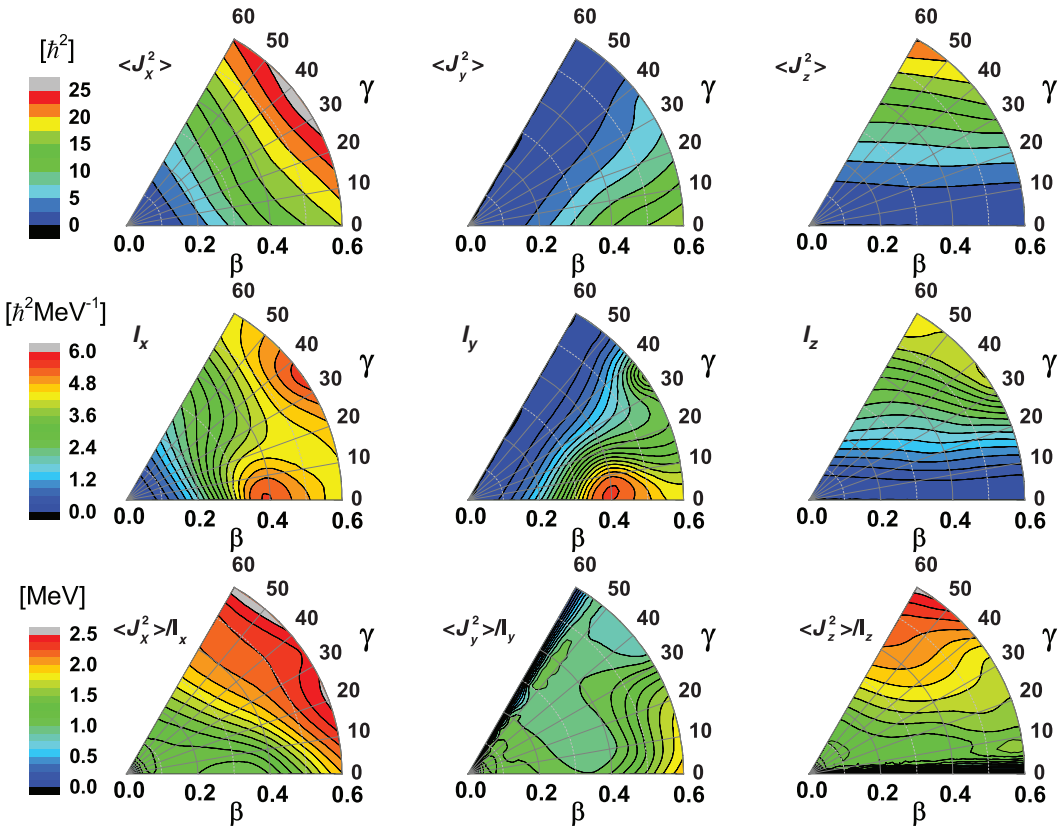

Fig. 4. Three components ($i = x, y, z$) for the expectation of the square of angular momentum $\langle \hat{J}_i^2 \rangle$, moment of inertia $\mathcal{I}_i$, and rotational correction energies $\langle \hat{J}_i^2 \rangle / \mathcal{I}_i$ of ^{38}Si in the β–γ plane, calculated with triaxial RMF wavefunctions.

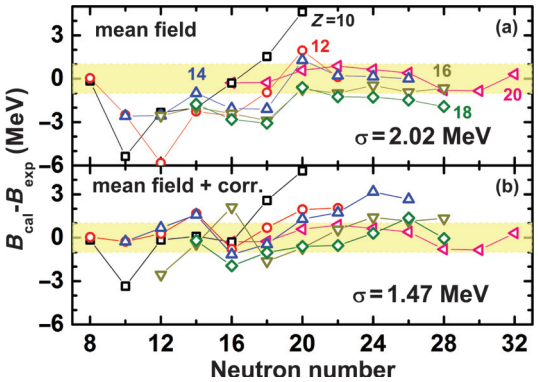

Fig. 5. Difference between calculated binding energies with the data [42] for even–even nuclei with proton numbers $10 \leq Z \leq 20$. The panels (a) and (b) represent the results with and without the phenomenological collective corrections calculated by Eq. (13), respectively.

state, it could appreciably increase the rotational correction energies, which is consistent with the observation in the exact AMP for triaxial states that the AMP has the tendency to lower the triaxial states [25,38,56].

Figure 5 displays the discrepancy of the calculated binding energies by PC-PK1 with the data for Ne, Mg, Si, S, Ar, and Ca isotopes. The upper and lower panels represent the results with and without the phenomenological collective corrections by Eq. (13), respectively. It is shown that most nuclei with $N < 20$ are underestimated by the pure mean-field calculations. Typical examples are ^{20}Ne and ^{24}Mg. This phenomenon has also been noticed in the previous RMF calculations [14,38]. After taking into account the energy corrections, the discrepancies in these nuclei are reduced significantly. The rms deviation in binding energies for the 41(50) nuclei ranging from Ne to Ar(Ca) is reduced from 2.22(2.02) MeV to 1.60(1.47) MeV. The remaining deviation is mainly contributed by the overbound nuclei ^{28,30}Ne, ^{32}Mg, and ^{34}Si; this requires further investigation. It should be noted that, after including the energy corrections, the rms deviation for 41 nuclei is almost the same irrespective of whether the triaxial deformation is taken into account or not, although the triaxiality has a significant effect on rotational correction energy. This is because the dynamic triaxial effect does indeed improve the description of binding energy for some nuclei, but also overestimates the binding energy of others. In addition, the main discrepancy between the present results and the previous results in Ref. [27] could be due to the consideration of the deformation dependence of vibrational correction in Ref. [27], as the effect of triaxial deformation is tiny and the same parameters of deformation dependence of rotational correction are adopted.

The differential of two-nucleon separation energies provides information on the neutron shell gap, which is given by [6,44]

$$\delta S_{2n}(Z, N) = 2B(Z, N) - B(Z, N-2) - B(Z, N+2), \tag{14}$$

where $B(Z, N)$ is the binding energy of nuclei with proton and neutron numbers Z and N respectively. Figure 6 displays the $N = 20$ shell gap obtained from the triaxial RMF calculations with and without the phenomenological collective corrections, in comparison with the results with restriction to spherical symmetry as well as the corresponding data. Compared with the spherical RMF calculation, the triaxially deformed RMF results are in better agreement with the data. In other words, deformation has a significant effect on the shell gap, as also discussed based on non-relativistic calculations in Ref. [55]. Except for $Z = 14$ and $Z = 20$, the shell gap has been reduced by 1–2 MeV.

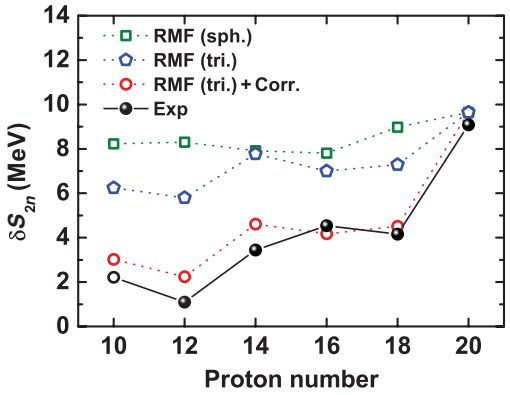

Fig. 6. The neutron shell gap at $N = 20$ from the triaxial RMF calculations using PC-PK1 without and with the phenomenological collective corrections by Eq. (13), in comparison with the spherical RMF calculations (sph.) and the corresponding data [42]. The open circle represents the data from extrapolation.

However, the pure mean-field results are still much larger than the data, in agreement with the RMF results using a meson-exchange force in Ref. [44]. Moreover, the data show that the size of the $N = 20$ shell gap is reduced significantly from about 9 MeV at the double-magic nucleus ^{40}Ca to about 2.2 MeV at ^{30}Ne, which has been well reproduced by the calculations with the collective correction energies. In short, both the deformation effect and phenomenological collective correction effect are very important to reproduce the neutron shell gap at $N = 20$. It should be noted that, as the $N = 18$, 20, and 22 nuclei have no triaxial deformation in the ground state, the deformation effect on the $N = 20$ shell gap is due to the quadrupole deformation.

4. Summary

In summary, we have carried out a systematic study of the ground states in even–even nuclei with $10 \leq Z \leq 20$ within the covariant density functional theory using the point-coupling force PC-PK1. The static effect of the triaxial deformation degree of freedom has been examined. We have found that ^{38}Si, ^{46}S, and ^{48}S exhibit considerable triaxial deformation, which is consistent with the previous triaxial RMF studies. The results indicate that the static effect from the triaxial deformation degree of freedom on the mean-field part of the nuclear binding energy in the present nuclei is marginal; however, it has a significant effect on the rotational correction energies. It is found that the rms deviation in binding energies for the 41 nuclei ranging from Ne to Ca is reduced from 2.22 MeV to 1.60 MeV and the evolution trend of the $N = 20$ shell gap is better reproduced after taking into account the phenomenological collective correction energies. In the future, a systematic study of the ground states of light nuclei at the beyond-mean-field level implemented with exact angular momentum projection [25,56] is required to confirm our findings. Apart from the light nuclei, the effect of triaxiality on medium and heavy nuclei should be investigated.

Acknowledgements

This work is supported by the NSFC (Grant Nos. 11105111, 11205068, 11305134, and 11475072), CPSC (Grant No. 2012M520667), the Basic Research Fund of Jilin University, and the National Major Scientific Instruments and Equipments Development Project (2012YQ24012102).

References

[1] I. Tanihata, H. Hamagaki, O. Hashimoto, Y. Shida, N. Yoshikawa, K. Sugimoto, O. Yamakawa, T. Kobayashi, and N. Takahashi, Phys. Rev. Lett. **55**, 2676 (1985).
[2] E. K. Warburton, J. A. Becker, and B. A. Brown, Phys. Rev. C **41**, 1147 (1990).
[3] I. Tanihata, D. Hirata, T. Kobayashi, S. Shimoura, K. Sugimoto, and H. Toki, Phys. Lett. B **289**, 261 (1992).
[4] O. Sorlin and M.-G. Porquet, Prog. Part. Nucl. Phys. **61**, 602 (2008).
[5] S.-G. Zhou, J. Meng, P. Ring, and E.-G. Zhao, Phys. Rev. C **82**, 011301(R) (2010).
[6] M. Bender, P.-H. Heenen, and P.-G. Reinhard, Rev. Mod. Phys. **75**, 121 (2003).
[7] G.-A. Lalazissis, P. Ring, and D. Vretenar, *Extended Density Functionals in Nuclear Structure Physics* (Springer, Berlin, 2004).
[8] M. Stoitsov, Phys. Part. Nucl. **41**, 868 (2010).
[9] P.-G. Reinhard, Rep. Prog. Phys. **52**, 439 (1989).
[10] P. Ring, Prog. Part. Nucl. Phys. **37**, 193 (1996).
[11] D. Vretenar, A. Afanasjev, G. Lalazissis, and P. Ring, Phys. Rep. **409**, 101 (2005).
[12] J. Meng, H. Toki, S. Zhou, S. Zhang, W. Long, and L. Geng, Prog. Part. Nucl. Phys. **57**, 470 (2006).
[13] T. Nikši, D. Vretenar, and P. Ring, Prog. Part. Nucl. Phys. **66**, 519 (2011).
[14] Z. Ren, Z. Zhu, Y. Cai, and G. Xu, Phys. Lett. B **380**, 241 (1996).
[15] D. Hirata, K. Sumiyoshi, I. Tanihata, Y. Sugahara, T. Tachibana, and H. Toki, Nucl. Phys. A **616**, 438 (1997).
[16] G. Lalazissis, A. Farhan, and M. Sharma, Nucl. Phys. A **628**, 221 (1998).
[17] G. Lalazissis, S. Raman, and P. Ring, At. Data Nucl. Data Tables **71**, 1 (1999).
[18] P. Möller, R. Bengtsson, B. G. Carlsson, P. Olivius, and T. Ichikawa, Phys. Rev. Lett. **97**, 162502 (2006).
[19] S. Cwiok, P.-H. Heenen, and W. Nazarewicz, Nature **433**, 705 (2005).
[20] W. Koepf and P. Ring, Nucl. Phys. A **493**, 61 (1989).
[21] D. Hirata, K. Sumiyoshi, B. Carlson, H. Toki, and I. Tanihata, Nucl. Phys. A **609**, 131 (1996).
[22] S. Sugimoto, K. Sumiyoshi, D. Hirata, B. Carlson, I. Tanihata, and H. Toki, [arXiv:9911025 [nucl-th]] [Search INSPIRE].
[23] J. Peng, H. Sagawa, S. Q. Zhang, J. M. Yao, Y. Zhang, and J. Meng, Phys. Rev. C **77**, 024309 (2008).
[24] J. Xiang, Z. P. Li, Z. Li, J. Yao, and J. Meng, Nucl. Phys. A **873**, 1 (2012).
[25] J. M. Yao, H. Mei, H. Chen, J. Meng, P. Ring, and D. Vretenar, Phys. Rev. C **83**, 014308 (2011).
[26] P. W. Zhao, Z. P. Li, J. M. Yao, and J. Meng, Phys. Rev. C **82**, 054319 (2010).
[27] Q. S. Zhang, Z. P. Li, J. M. Yao, Z. M. Niu, and J. Meng, Front. Phys. **9**, 529 (2014).
[28] B. A. Nikolaus, T. Hoch, and D. G. Madland, Phys. Rev. C **46**, 1757 (1992).
[29] T. Büvenich, D. G. Madland, J. A. Maruhn, and P.-G. Reinhard, Phys. Rev. C **65**, 044308 (2002).
[30] S. Krieger, P. Bonche, H. Flocard, P. Quentin, and M. Weiss, Nucl. Phys. A **517**, 275 (1990).
[31] M. Bender, K. Rutz, P. G. Reinhard, and J. Maruhn, Eur. Phys. J. A **8**, 59 (2000).
[32] J. Xiang, Z. P. Li, J. M. Yao, W. H. Long, P. Ring, and J. Meng, Phys. Rev. C **88**, 057301 (2013).
[33] M Anguiano, A M Lallena, G Co', and V De Donno, J. Phys. G: Nucl. Part. Phys. **41**, 025102 (2014).
[34] A.V. Afanasjev, S.E. Agbemava, D. Ray, and P. Ring, Phys. Lett. B **726**, 680 (2013).
[35] X. Y. Qu, Y. Chen, S. Q. Zhang, P. W. Zhao, I. J. Shin, Y. Lim, Y. Kim, and J. Meng, Sci. China Phys. Mech. Astron. **56**, 2031 (2013).
[36] P. Zhao, B. Sun, and J. Meng, Chin. Phys. Lett. **26**, 112102 (2009).
[37] P. Ring and P. Shuck, *Nuclear Many Body Problem* (Springer, Berlin, 1980).
[38] J. M. Yao, J. Meng, P. Ring, and D. P. Arteaga, Phys. Rev. C **79**, 044312 (2009).
[39] Z. P. Li, J. M. Yao, D. Vretenar, T. Niksic, H. Chen, and J. Meng, Phys. Rev. C **84**, 054304 (2011).
[40] Y. Sugahara and H. Toki, Nucl. Phys. A **579**, 557 (1994).
[41] J. P. Delaroche, M. Girod, J. Libert, H. Goutte, S. Hilaire, S. Péru, N. Pillet, and G. F. Bertsch, Phys. Rev. C **81**, 014303 (2010).
[42] G. Audi, A. H. Wapstra, and C. Thibault, Nucl. Phys. A **729**, 337 (2003).
[43] Yu. E. Penionzhkevich, Hyperfine Interact. **171**, 157 (2006).
[44] B. H. Sun and J. Li, Chin. Phys. C **32**, 11 (2008).
[45] J. Erler, N. Birge, M. Kortelainen, W. Nazarewicz, E. Olsen, A. Perhac, and M. Stoitsov, J. Phys.: Conf. Ser. **402**, 012030 (2012).
[46] D. R. Inglis, Phys. Rev. **103**, 1786 (1956).

[47] S. Belyaev, Nucl. Phys. **24**, 322 (1961).
[48] Z. P. Li, T. Niksic, P. Ring, D. Vretenar, J. M. Yao, and J. Meng, Phys. Rev. C **86**, 034334 (2012).
[49] M. Samyn, S. Goriely, M. Bender, and J. M. Pearson, Phys. Rev. C **70**, 044309 (2004).
[50] S. Goriely, M. Samyn, J. M. Pearson, and M. Onsi, Nucl. Phys. A **750**, 425 (2005).
[51] N. Chamel, S. Goriely, and J. M. Pearson, Nucl. Phys. A **812**, 72 (2008).
[52] J. Libert, M. Girod, and J. P. Delaroche, Phys. Rev. C **60**, 054301 (1999).
[53] Y. Fu, H. Mei, J. Xiang, Z. P. Li, J. M. Yao, and J. Meng, Phys. Rev. C **87**, 054305 (2013).
[54] M. Bender, G. F. Bertsch, and P.-H. Heenen, Phys. Rev. C **73**, 034322 (2006).
[55] M. Bender, G. F. Bertsch, and P.-H. Heenen, Phys. Rev. C **78**, 054312 (2008).
[56] J. M. Yao, J. Meng, P. Ring, and D. Vretenar, Phys. Rev. C **81**, 044311 (2010).